Structural Engineering and Mechanics, Vol. 33, No. 6 (2009) 765-779
DOI: http://dx.doi.org/10.12989/sem.2009.33.6.765

Damage assessment of reinforced concrete beams including the load environment

X.Q. Zhu†

School of Engineering, The University of Western Sydney, Kingswood Campus, NSW 1797, Australia

S.S. Law‡

Civil and Structural Engineering Department, The Hong Kong Polytechnic University, Hunghom, Kowloon, Hong Kong, P. R. China

H. Hao‡†

School of Civil and Resource Engineering, The University of Western Australia, Crawley, WA 6009, Australia

(Received January 9, 2007, Accepted October 14, 2009)

Abstract. Quantitative condition assessment of structures has been traditionally using proof load test leading to an indication of the load-carrying capacity. Alternative approaches using ultrasonic, dynamics etc. are based on the unloaded state of the structure and anomalies may not be fully mobilized in the load resisting path and thus their effects are not fully included in the measured responses. This paper studies the effect of the load carried by a reinforced concrete beam on the assessment result of the crack damage. This assessment can only be performed with an approach based on static measurement. The crack damage is modelled as a crack zone over an area of high tensile stress of the member, and it is represented by a damage function for the simulation study. An existing nonlinear optimization algorithm is adopted. The identified damage extent from a selected high level load and a low load level are compared, and it is concluded that accurate assessment can only be obtained at a load level close to the one that creates the damage.

Keywords: reinforced concrete; beam; damage; assessment; inverse problem; finite element; crack; static load; deflection.

1. Introduction

Previous study in the condition assessment of aging reinforced concrete bridge deck (Law *et al.*, 1995) revealed a consistent pattern of crack zones in the bridge beams after years of service. Cerri

† Lecturer, Corresponding author, E-mail: xinqun.zhu@uws.edu.au
‡ Associate Professor
‡† Professor

and Vestroni (2000) modelled the damage zone as a beam element with a reduced flexural stiffness with three parameters to define the damage, i.e., the position, the extent of the damage and the reduction of the elemental flexural stiffness. Wahab *et al.* (1999) also proposed another set of parameters to describe the damage zone in reinforced concrete beams, which are, the length of the damage zone, its magnitude and the variation of the damage magnitude from the centre to the end of the damage zone. Maeck *et al.* (2000) presented two techniques to calculate the stiffness degradation of the damaged reinforced concrete beam based on this damage model from the experimental modal characteristics.

Qualitative condition assessment of reinforced concrete structures has been traditionally using proof load test leading to an indication of the load-carrying capacity. Dynamics approach is very popular nowadays to identify local damages, but it does not give any clue on the associated load-carrying capacity of the structure. However the dynamics approach and other alternative approaches of condition assessment are based on the unloaded state of the structure and local anomaly may not be fully mobilized in the load resisting path and thus their effects are not fully included in the measured responses. The identified results would be an under-estimation of the true value.

This paper addresses the question on whether the identified results obtained by inverse analysis from a low-level load test representative of the actual damage carried by the structure. The process of damage detection is conducted on a reinforced concrete beam where local damage is created experimentally under static loading and the crack damage is assessed in an inverse analysis with an existing nonlinear optimization algorithm. The crack damage is modelled with the Wahab three-parameters model as a cracked zone represented by a damage function. Unlike results obtained for structures of isotropic homogeneous material, the identified damage extent of the reinforced concrete beam is found dependent on the static load it carries. The identified damage state of the beam using a low level loading is found in general less severe than the damage state created by static load at a higher load level. It is concluded that accurate assessment of the crack damage in a reinforced concrete beam is only possible with an identification load close to the one that creates the damage.

1.1 Damage function for the reinforced concrete beam

Cracks in reinforced concrete beam will not be modeled individually but as a smeared zone of cracks instead. The three-parameter model proposed by Wahab *et al.* (1999) is adopted which models the damage effect as a distribution of reduction in the flexural rigidity of the cross-section as

$$EI(x) = E_0 I\left\{1 - \gamma\cos^2\left[\frac{\pi}{2}\left(\frac{|x-l_c|}{\beta L/2}\right)^n\right]\right\} \quad (l_c - \beta L/2 < x < l_c + \beta L/2) \tag{1}$$

where γ, β, n are the damage parameters. l_c is the position of the mid-point of the damage zone, and L is the length of beam. The parameter β characterizes the length of the damaged zone with $0.0 \le \beta \le 1.0$. Parameter γ characterizes the magnitude of the damage with $0.0 \le \gamma \le 1.0$. No damage exists if γ equals to 0.0. When γ equals to 1.0, the flexural rigidity vanishes at the mid-point of the damage zone. Parameter n characterizes the variation of the flexural rigidity from the mid-point of the damage zone to the ends of the beam. E_0 is the original elastic modulus of the beam without damage.

The averaged flexural stiffness of the ith element of the beam that carries the damage can be formulated as a function of the three parameters as

$$\tilde{E}I = \begin{cases} E_0 I & il_e < l_c - \beta L/2 \text{ or } (i-1)l_e > l_c + \beta L/2 \\ \dfrac{E_0 I}{l_e}\left[\int_{(i-1)l_e}^{l_c - \beta L/2} dx + \int_{l_c - \beta L/2}^{l_c + \beta L/2}\left(1 - \gamma\cos^2\left(\dfrac{\pi}{2}\left(\dfrac{|x-l_c|}{\beta L/2}\right)^n\right)\right)dx + \int_{l_c + \beta L/2}^{il_e} dx\right], & \\ \qquad (i-1)l_e < l_c - \beta L/2 \text{ and } il_e > l_c + \beta L/2 & \\ \dfrac{E_0 I}{l_e}\left[\int_{(i-1)l_e}^{l_c - \beta L/2} dx + \int_{l_c - \beta L/2}^{il_e}\left(1 - \gamma\cos^2\left(\dfrac{\pi}{2}\left(\dfrac{|x-l_c|}{\beta L/2}\right)^n\right)\right)dx\right], & \\ \qquad (i-1)l_e < l_c - \beta L/2 \text{ and } il_e < l_c + \beta L/2 & \\ \dfrac{E_0 I}{l_e}\int_{(i-1)l_e}^{il_e}\left(1 - \gamma\cos^2\left(\dfrac{\pi}{2}\left(\dfrac{|x-l_c|}{\beta L/2}\right)^n\right)\right)dx, & (i-1)l_e > l_c - \beta L/2 \text{ and } il_e < l_c + \beta L/2 \\ \dfrac{E_0 I}{l_e}\left[\int_{(i-1)l_e}^{l_c + \beta L/2}\left(1 - \gamma\cos^2\left(\dfrac{\pi}{2}\left(\dfrac{|x-l_c|}{\beta L/2}\right)^n\right)\right)dx + \int_{l_c + \beta L/2}^{il_e} dx\right], & \\ \qquad (i-1)l_e > l_c - \beta L/2,\ (i-1)l_e < l_c + \beta L/2 \text{ and } il_e > l_c + \beta L/2 & \end{cases}$$

$$(i = 1, 2, \ldots, N) \tag{2}$$

where l_e is the length of the finite element.

Note that the above equation refers to five states of a finite element defined as follows:

The 1st line of Eq. (2) refers to the ith element which is outside the range of the damage zone.

The 2nd line refers to the ith element which is larger than the damage zone and it takes the whole damage inside the element.

The 3rd line refers to the damage zone which lies partly (left part of the damage) on the ith element and partly (right part of the damage) on the (i+1)th element.

The 4th line refers to the ith element which is smaller than the damage zone and completed within the damage zone.

The 5th line is similar to the 3rd line and refers to the damage zone which lies partly (right part of the damage) on the ith element and partly (left part of the damage) on the (i-1)th element.

The damage index of a finite element can be determined from the average EI of the element as

$$\text{Damage index of the } i\text{th element, } \alpha_i = 1 - \frac{\tilde{E}I_i}{EI_i}$$

1.2 elemental damage Index

In the inverse problem of damage identification, it is assumed that the stiffness matrix of the whole element decreases uniformly with damage, and the flexural rigidity, EI_i, of the ith finite element of the beam becomes $(1-\alpha_i)EI_i$ when there is a damage. The fractional change in stiffness of an element can also be expressed as

$$\Delta\mathbf{K}_i = (\overline{\mathbf{K}}_i - \tilde{\mathbf{K}}_i) = \alpha_i \overline{\mathbf{K}}_i \tag{3}$$

where $\overline{\mathbf{K}}_i$ is the stiffness matrix of the ith element of the undamaged beam and $\tilde{\mathbf{K}}_i$ is the stiffness matrix of the ith element of the damaged beam by Eq. (2). $\Delta\mathbf{K}_i$ is the stiffness reduction of the element. A positive value of $\alpha_i \in [0, 1]$ indicates a loss in the element stiffness.

The stiffness matrix of the damaged structure is an assembly of all the element stiffness matrix $\tilde{\mathbf{K}}_i$

$$\tilde{\mathbf{K}} = \sum_{i=1}^{N} \mathbf{A}_i^T \tilde{\mathbf{K}}_i \mathbf{A}_i = \sum_{i=1}^{N} (1-\alpha_i) \mathbf{A}_i^T \overline{\mathbf{K}}_i \mathbf{A}_i \tag{4}$$

where $\mathbf{A}_i$ is the transformation matrix that facilitates automatic assembling of the global stiffness matrix from the constituting element stiffness matrix.

1.3 Damage identification from displacement measurements

The force-displacement relation of a damaged structure can be expressed as

$$F = \tilde{K}\tilde{U} = (K - \Delta K)(\overline{U} - \Delta U) \tag{5}$$

where $\mathbf{F}$ is the force vector. $\mathbf{F} = \Phi\mathbf{P}$ is the force vectors, in which $\mathbf{P} = \{P_1, P_2, \ldots, P_{Np}\}^T$ is the vector of static loads; $\Phi = \{\Phi_1\ \Phi_2\ \ldots\ \Phi_l\ \ldots \Phi_{Np}\}$ is a $2(N+1)\times N_p$ shape function matrix, N_p is the number of loads.

$\overline{\mathbf{U}}$ and $\tilde{\mathbf{U}}$ are the vectors of nodal deformation without and with damage, and $\Delta\mathbf{U} = \overline{\mathbf{U}} - \tilde{\mathbf{U}}$ is the vector of deformation difference due to damage. When under the same applied load, Eq. (5) indicates qualitatively that a reduction in the stiffness matrix corresponds to an increase in the vector of deformations.

Vector $\Delta\mathbf{U}$ can be estimated from Eq. (5) as

$$\Delta U = -K^{-1}\Delta K K^{-1} F + K^{-1}\Delta K \Delta U \approx -K^{-1}\Delta K K^{-1} F \tag{6}$$

by neglecting the second order terms. Substituting the force displacement relation of the intact structure and the stiffness matrix of the damage structure into Eq. (6), the analytical vector of deformation due to damage is obtained as

$$\Delta U \approx \sum_{i=1}^{N} \alpha_i K^{-1} A_i^T K_i A_i K^{-1} \Phi P = \sum_{i=1}^{N} \alpha_i \hat{U}_i \tag{7}$$

where $\hat{U}_i = K^{-1} A_i^T K_i A_i K^{-1} \Phi P$, and $\mathbf{A}_i$ is the transformation matrix for the ith element for assembling the global stiffness matrix from the constituting element stiffness matrix.

The measured displacement u_s at location x_s can be obtained from the shape functions $\boldsymbol{\varphi}_s$ and nodal displacement $\mathbf{u}$ of the beam as

$$u_s = \boldsymbol{\varphi}_s \mathbf{u} \tag{8}$$

with

$$(j-1)l_e \le x_s < j l_e$$

$$\varphi_s = \{0, 0, \ldots, 0, \varphi_j, 0, \ldots, 0\}$$

and

$$\varphi_j = \left\{1 - 3\left(\frac{x}{l_e}\right)^2 + 2\left(\frac{x}{l_e}\right)^3, x\left(\frac{x}{l_e} - 1\right)^2, 3\left(\frac{x}{l_e}\right)^2 - 2\left(\frac{x}{l_e}\right)^3, x\left(\frac{x}{l_e}\right)^2 - \frac{x^2}{l_e}\right\}$$

$$x = x_s - (j-1)l_e$$

For N_s measuring points at $\{x_s, s = 1, 2, \ldots, N_s\}$, Eq. (8) can be written as follows

$$\mathbf{U}_s = \Phi_s \mathbf{U} \tag{9}$$

where $\mathbf{U}_s = \{u_1, u_2, \ldots, u_{N_s}\}^T$ and $\boldsymbol{\Phi}_s = \{\varphi_1, \varphi_2, \ldots, \varphi_{N_s}\}^T$

The error between the vectors of difference between the calculated and measured deformations of the structure is obtained from Eqs. (7) and (9) as

$$e(\boldsymbol{\alpha}) = \boldsymbol{\Phi}_s \Delta \mathbf{U} - \Delta \mathbf{U}_s \tag{10}$$

where $\Delta \mathbf{U}_s$ is the vector of differences between the measured displacement of structures with and without damage.

The algorithm to identify the damage is based on minimizing the least-squares error function in Eq. (10) as (Wang *et al.* 2001)

$$\text{Minimize} \quad J(\boldsymbol{\alpha}) = \frac{1}{2}\|e(\boldsymbol{\alpha})\|^2 = \frac{1}{2}\left\|\sum_{i=1}^{N} \alpha_i \boldsymbol{\Phi}_s \hat{U}_i - \Delta \mathbf{U}_s\right\|^2$$

$$\text{subject to} \quad 0 \le \alpha_i \le 1, \quad (i = 1, 2, \ldots, N) \tag{11}$$

This model can be cast into the following quadratic programming problem (Bannan and Hjelmstad 1994a) for determining the damage indices

$$\text{Minimize} \quad J(\alpha) = \frac{1}{2}\alpha^T K^T \Phi_s^T \Phi_s \alpha K - \Delta U_s^T \Phi_s \alpha K + \frac{1}{2}\Delta U_s^T \Delta U_s$$

$$\text{subject to} \quad 0 \le \alpha_i \le 1, \quad (i = 1, 2, \ldots, N) \tag{12}$$

where $\boldsymbol{\alpha} = \{\alpha_i\}^T$. The algorithm presented by Goldfarb and Idnani (1983) is used to solve this quadratic programming problem. Detail of the iterative algorithm used to solve the nonlinear optimization problem is listed as follows:

1) Calculate the matrix $\boldsymbol{\Phi}_s = \{\varphi_1, \varphi_2, \ldots, \varphi_{N_s}\}^T$, $\Phi = \{\Phi_1\ \Phi_2\ \ldots\ \Phi_l\ \ldots \Phi_{Np}\}$.
2) Initially assume that there is no damage in the beam, i.e., $\boldsymbol{\alpha}_0 = \{0, 0, \ldots, 0\}^T$.
3) Since we cannot measured the deformation of the intact beam under a given load for a reinforced concrete beam (the beam will naturally crack under load), the baseline deformation vector of the structure without damage $\overline{\mathbf{U}}_s$ is calculated and used instead of the measured deformation vector from the intact beam, and the initial vector of measured deformation difference from the intact and damage beams is obtained as $\Delta \mathbf{U}_{s0} = \overline{\mathbf{U}}_s - \mathbf{U}_s$.
4) Identify damage index $\mathbf{a}_j$ using Eq. (12). $j = 1$ for the first cycle of iteration.
5) Calculate $\Delta \mathbf{U}$ by Eq. (7) with the updated $\boldsymbol{\alpha} = \boldsymbol{\alpha}_j + \boldsymbol{\alpha}_0$ and $\mathbf{U}_{\mathrm{Re}\,constructed} = \overline{\mathbf{U}}_s - \boldsymbol{\Phi}_s \Delta \mathbf{U}$.
6) Calculate the following criteria of convergence

$$\begin{cases} Error1 = \dfrac{\|\mathbf{U}_s - \mathbf{U}_{\mathrm{Re}\,constructed}\|}{\|\mathbf{U}_s\|} \times 100\% \\[2ex] Error2 = \dfrac{\|\boldsymbol{\alpha}_{j+1} - \boldsymbol{\alpha}_j\|}{\|\boldsymbol{\alpha}_j\|} \times 100\% \end{cases} \tag{13}$$

α_j, α_{j+1} are the identified damage indices in two successive iterations. Convergence is achieved when both errors are less than the pre-defined tolerance values.

7) When the computed error does not converge, calculate $\Delta\mathbf{U}_s = \mathbf{U}_{\mathrm{Re}\,constructed} - \mathbf{U}_s$ and $\alpha_0 = \alpha$. Repeat Steps 4 to 6 until convergence is reached.

The damage identification is performed iteratively. The initial value of the damage index is assumed as zero. The difference between the measured and the calculated baseline deformation is used to identify the local damages by Eq. (12), and then the deformation from the improved finite element model of the beam under the same set of applied load is reconstructed. The difference between the reconstructed and measured deformations is again used to update the finite element model of the beam until the convergence criteria of Eq. (13) is achieved.

2. Numerical simulations

2.1 Example 1: A reinforced concrete beam with damage in a single element

A numerical example with a four metre long simply supported uniform rectangular concrete beam is studied. It has a 300 mm high and 200 mm wide cross-section and 3.8 m clear span. There are three 20 mm diameter mild steel bars at the bottom of the beam corresponding to a steel percentage of 1.57%, and two 6 mm diameter steel bars at the top of the beam section. 6 mm diameter mild steel links are provided at 195mm spacing over the whole beam length. The density, tensile strength, Young's modulus, and Poisson's Ratio of concrete are respectively 2351.4 kg/m^3, 3.77 MPa, 30.2 GPa and 0.16. The Young's Modulus and yield stress of the mild steel bars are respectively 181.53 GPa and 300.07 MPa. All the above parameters are measured from experiment. This study is to verify the identification algorithm and a local damage in the form of stiffness reduction in a single finite element is used.

2.2 Study 1: Verification of the damage identification algorithm

The beam is discretized into eight elements. Damage is located at the third element and modelled with α_3 = 0.1. The location of the damage is intentionally selected to avoid symmetry of the measured information which may lead to a set of non-unique identified results. A static load of

Table 1 Displacements (mm) at different locations under the static load

Load location / Measuring location	1/3L		1/2L		3/4L	
	$\overline{U}_s$	U_s	$\overline{U}_s$	U_s	$\overline{U}_s$	U_s
1/8L	0.10	0.10	0.10	0.10	0.06	0.06
1/4L	0.18	0.19	0.18	0.19	0.11	0.12
3/8L	0.23	0.24	0.25	0.25	0.16	0.16
1/2L	0.23	0.23	0.28	0.28	0.19	0.19
5/8L	0.20	0.20	0.26	0.26	0.20	0.20
3/4L	0.15	0.15	0.19	0.19	0.17	0.17
7/8L	0.08	0.08	0.10	0.10	0.10	0.10

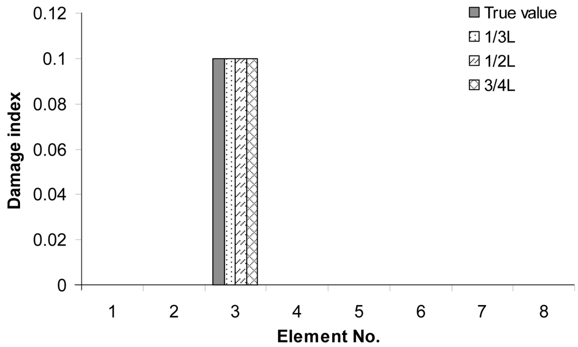

Fig. 1 Identified results from using different load locations

5000 N is applied to the beam at $1/3L$, $1/2L$ or $3/4L$ separately. Seven displacement measurements evenly distributed along the beam are used for the identification. The Young's modulus of material of each element is taken as the unknown. Table 1 shows the measuring locations and their values. The tolerance values for *Error*1 and *Error*2 are 0.01 in the simulations and the result converges after 21 iterations. Fig. 1 shows the identified results from the three load cases. The identified results are very close to the true value. This shows that the proposed damage identification algorithm is reliable and accurate results can be obtained from the static response measurements.

2.3 Study 2: Effect of noise in measurement

One percentage white noise is added to the calculated displacements of the beam to simulate the polluted measurements with

$$U_s = U_{calculated}(1 + E_p * N_{noise}) \tag{14}$$

where U_s and $U_{calculated}$ are the polluted and the original "measured" displacements. E_p is the noise level and $\mathbf{N}_{noise}$ is a standard normal distribution vector with zero mean value and unit standard deviation, and it is generated independently for each component of the measured displacement.

The parameters are the same as in the above study with the load located at $1/2L$. Monte Carlo method is used in the simulations. One hundred sets of simulated results are obtained. Figs. 2(a) and (c) shows the relation between the mean values of the identified results for Element 3 and the number of simulations when the damage index α_3 is 0.1 and 0.3, separately. This corresponds to State 2 of Eq. (2) where only element 3 has a 10% and 30% in the flexural stiffness respectively. Figs. 2(b) and (d) show their histograms compared with the corresponding normal distributions. In Figs. 2(a) and (c), the mean values of the identified damage indices converge to a constant value when the number of simulations is larger than 80. In Figs. 2(b) and (d), the histograms of the identified results are close to the normal distribution. These results indicate the estimated damage indices have normal distributions approximately if the displacement measurement noise follows a normal distribution. More simulated results would give a more clear indication of distribution with the damage indices.

Fig. 3 shows the range of identified results from 1% noise polluted static responses when the damage index α_3 is 0.1 and 0.3, separately. In practice, static measurement is more accurate than dynamic measurements, and 1% simulated noise pollution is considered good enough to represent

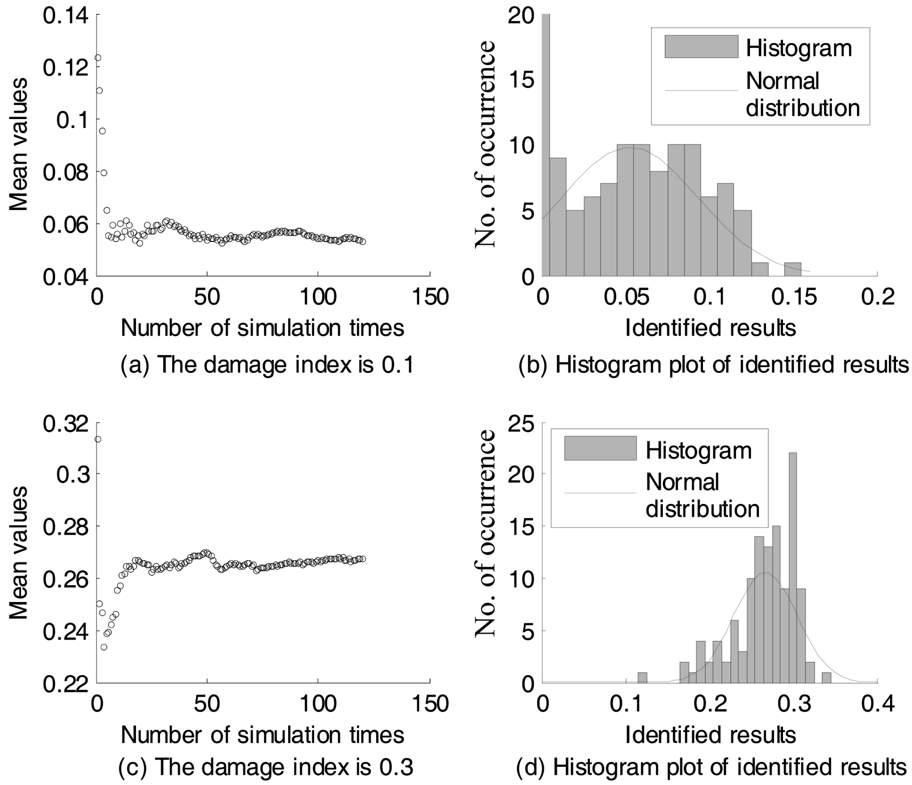

(a) The damage index is 0.1
(b) Histogram plot of identified results
(c) The damage index is 0.3
(d) Histogram plot of identified results

Fig. 2 The identified results for element 3 in the simulations

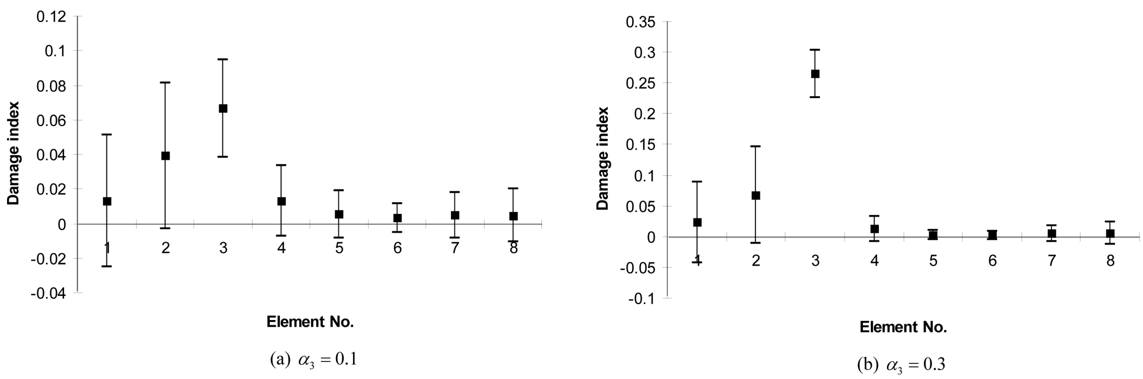

(a) $\alpha_3 = 0.1$
(b) $\alpha_3 = 0.3$

Fig. 3 Identified results from 1% noise polluted static responses; (■) denotes the mean value, (|——|) denotes the range of standard deviation.

the random error with real static measurements. The damage location and extent can be determined accurately for the large damage case of α_3 = 0.3 but not for the small damage case. The identified results for Elements 2 and 3 overlap for the small damage case of α_3 = 0.1. The predicted mean and standard deviation of the identified results show a large variation in the adjacent elements close to the left support, and a smaller variation in all other elements. This statistical approach adds more information to the behaviour of the identified damage of the structure with polluted measurement.

Table 2 Damage indices from different number of sensor and finite element discretization

Element number	Equivalent damage indices	Identified damage indices					
		Number of sensors			Number of finite elements		
		7	15	32	4	8	16
1	0.00	0.00	0.00	0	0.03	0.01	0.00
2	0.00	0.00	0.00	0	0.03	0.01	0.00
3	0.00	0.00	0.00	0	0.03	0.04	0.00
4	0.01	0.12	0.21	0	0.03	0.04	0.12
5	0.38	0.28	0.15	0.434	0.27	0.43	0.28
6	0.49	0.57	0.55	0.451	0.27	0.43	0.57
7	0.22	0.00	0.18	0.236	0.27	0.11	0.00
8	0.00	0.06	0.01	0	0.27	0.11	0.06
9	0.00	0.00	0.00	0	0.00	0.00	0.00
10	0.00	0.00	0.00	0	0.00	0.00	0.00
11	0.00	0.00	0.00	0	0.00	0.00	0.00
12	0.00	0.00	0.00	0	0.00	0.00	0.00
13	0.00	0.03	0.00	0	0.01	0.01	0.03
14	0.00	0.00	0.00	0	0.01	0.01	0.00
15	0.00	0.00	0.00	0	0.01	0.00	0.00
16	0.00	0.00	0.00	0	0.01	0.00	0.00

2.4 Example 2: A reinforced concrete beam with a damage zone

Since this study is on the effect of static load on the identification of system parameters, the effect of other parameters should preferably be removed. Therefore, before applying the above technique to the experimental reinforced concrete beam, a study is made on the optimal number of sensors and finite element discretization required for an accurate assessment. A concentrated load of 5000 N is applied at mid-span of the beam. The damage zone is defined by the three-parameter model with $l_c = L/3$, $\beta = 0.2$, $\gamma = 0.5$ and $n = 2$. The equivalent set of damage indices in the different beam elements are shown in column 2 of Table 2. The damage index in each beam element is taken as the unknown in the identification.

2.5 Study 3: Optimal number of sensors

The beam is discretized into 16 finite elements, and 7, 15 and 31 number of displacement "measurement" recorded at equal spacing along the beam are separately used in the identification. The identified results are compared with the true equivalent damage indices of 0.1 and 0.3 in the second column of Table 2. The error, *Error2,* defined in Eq. (13) for 7, 15 and 31 displacement readings are 25.3%, 18.1% and 7.0%, respectively. The results show that higher accuracy is achieved with more sensors, while results from seven sensors are considered acceptable.

2.6 Study 4: Optimal finite element discretization

The beam is discretized into four, eight and sixteen finite elements in turn for the identification. Seven measured displacements recorded at equal spacing along the beam are used. The identified results are shown in Table 2, and the errors, Error2, defined in Eq. (13) are 33.9%, 16.6% and 25.9%, respectively for the 4, 8 and 16 elements discretization configuration. The results show that the accuracy of the identified damage indices is higher with increasing number of finite elements, and eight finite elements are considered giving acceptable results when there are seven measurements. The 16 element configuration gives poorer results than the 8 element configuration when only seven transducers are used. When looking at results from this and the last studies, it may be concluded that more sensor would give more spatial information on the damage location in the structure and the benefit of having a more refined finite element model would be realized only when the number of sensor be increased to the maximum with one sensor at each internal node of the beam.

3. Laboratory study

The 4 m length beam described in the numerical study is test as shown in Fig. 4(a). The beam was simply supported on two 50 mm diameter steel bars 3.8 m apart. The steel bars lie on top of a solid steel support fixed to a large concrete block on the strong floor of the laboratory. A piece of thin rubber pad is placed between the steel bar and the bottom of the concrete beam for level

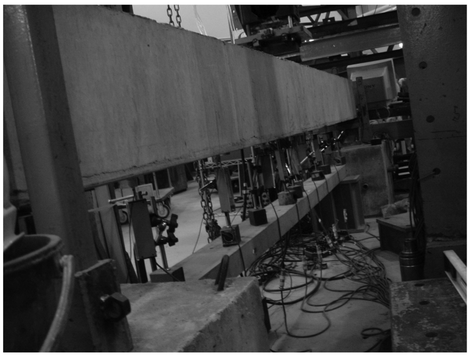

(a) Experimental system

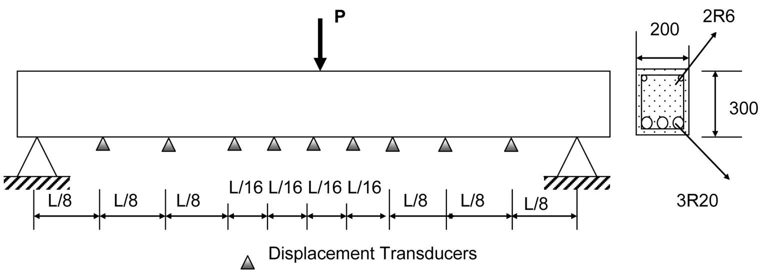

(b) Sensor location

Fig. 4 Reinforced concrete beam and sensor locations

Table 3 Load Level in different loading stages

Load stage	1	2	3	4	5	6	7	8
Assessment load (kN)	10	17	25	35	45	50	55	60
Maximum load (kN)	15	25	35	45	50	55	60	67

Table 4 Cracks in each element at the end of the final loading stage

Element No.		4	5	6	7	8	9	10	11	12	13
Front view	No. of cracks	1	1	1	1	2	2	1	2	1	1
	Length (mm)	162	162	150	177	163, 211	211, 192	181	141, 137	163	171
Back view	No. of cracks	-	1	1	1	2	2	-	-	-	-
	Length (mm)	-	161	170	145	180, 160	160, 202	-	-	-	-

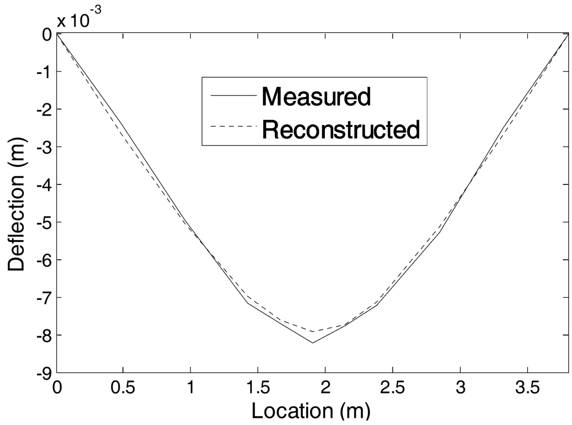

Fig. 5 Comparison of deflections at midspan at 60 kN

adjustment. The vertical stiffness of the rubber pad was measured as 39.41 kN/mm after the test and it will be used to modify the measured displacements.

The initial flexural rigidity of the concrete beam is estimated by direct calculation using the measured material property and the geometrical dimensions of the beam. The beam carries no crack and therefore the steel bars insides are not considered contributing as a composite component of the beam. The beam was incrementally loaded at mid-span to create crack damage using three-point loading. Eight loading cycles starting from 0.0 kN to a specified load level as shown in Table 3 were conducted. The load was subsequently unloading after reaching the maximum. After unloading in the last loading cycle from 67 kN, the beam was loaded up to failure by yielding of steel bars at 75 kN. The crack locations and lengths were recorded in addition to the displacement measurements and they are shown in Table 4.

The beam is divided into eight and sixteen finite elements for the study. First crack appears in elements 8 and 9 at 17 kN in the sixteen finite element model. Nine displacement transducers are located at the bottom of the beam to measure the deflection under load as shown in Fig. 4(b). The static responses at all the nine measurement points are used in the damage identification. The INV300 data acquisition system is used to record data from all the 9 displacement sensors and the applied load with a sampling rate of 200.12 Hz.

Fig. 5 compares the measured and reconstructed deflection at midspan of the beam at 60 kN in the final load stage. The reconstructed deflection is from the beam incorporating the identified damage indices α. The two curves are very close to each other and nearly symmetrical about the mid-span of the beam. This is consistent with the small error (results not shown) between the two curves calculated by the following formula.

$$Error = \frac{\| U_s - U_{Reconstructed} \|}{\| U_s \|} \times 100\% \tag{15}$$

By Eq. (15), the difference between the measured and reconstructed responses at 60 kN is 2.53%.

3.1 Damage identification – study on the damage evolution under load

Firstly, the displacement in a subsequent loading stage with an assessment load close to the maximum load of the previous stage is used to identify the damage. For example, the displacement at an assessment load of 45 kN in the sixth loading stage is used to assess the damage created by the same load at the fifth loading stage. This is to simulate the real practice of assessment at a second loading cycle instead of the same load cycle. The assessment load for each load stage is shown in Table 3. Elements 4 and 5 are identified to have damage in the case of the 8 finite element model, while elements 8, 9 and 11 are identified to have damage in the 16 finite element model. The identified damage indices are plotted in Figs. 6(a) and 6(b) indicating a nonlinear increase with an increase in the applied load. The element numbers are marked as (•) beside the

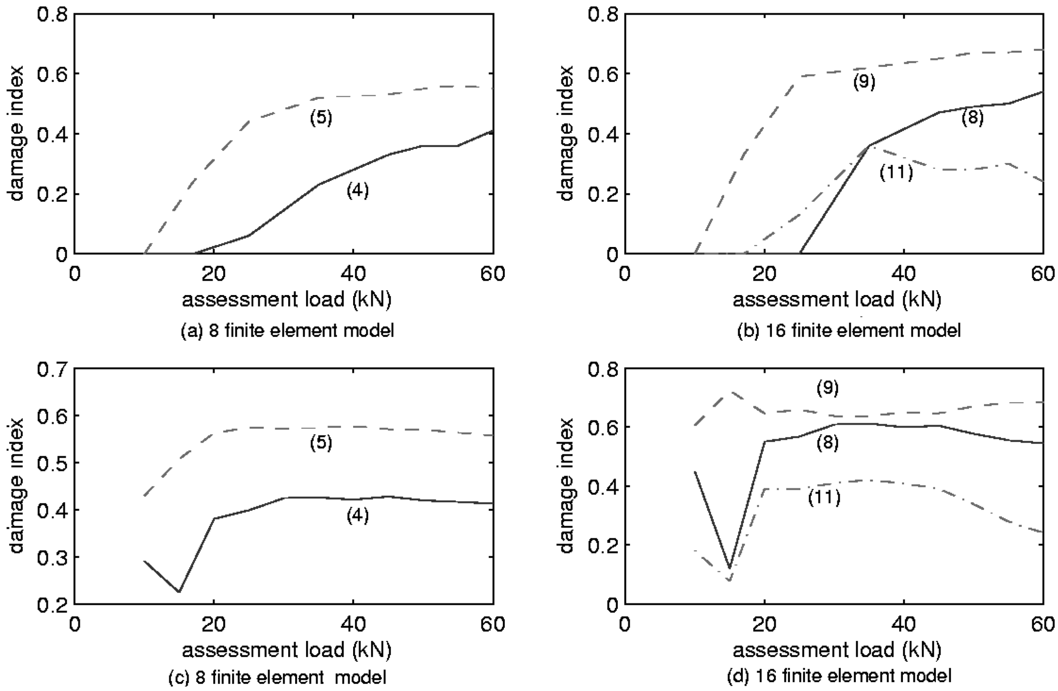

Fig. 6 Identified damage indices. (a), (b) evolution with load; (c), (d) after the final loading stage

curves. In Figs. 6(a) and (c), the blue solid line with the legend (4) is the identified damage indices for Element 4, and the red dashed line with the legend (5) is the identified damage indices for Element 5. In Figs. 6(b) and (d), the blue solid line with the legend (8), the red dashed line with the legend (9), and the red dashed-dot line with the legend (11) are the identified damage indices for Elements 8, 9 and 11, respectively.

The curve flattens at around 35 kN for element 5 and 45 kN for element 4. This is because part of the deformation does not recover after unloading in the previous load cycle and the damage index would be an underestimation of the true value. Table 4 shows the dimensions and locations of cracks in the sixteen finite element model when the beam was loaded up to 67 kN. It is noted that the damage is more or less symmetrical about the midspan, and the crack damage in the right halve of the beam is slightly more severe than the left halve. Elements 8, 9 and 11 are identified to have damage as shown in Fig. 6(b). It should be noted that Figs. 6(a) and 6(b) are damage evolution diagrams of the damaged elements with load. Each data point on the curve corresponds to the damage created by the associated load. After the beam was loaded up to 60 kN in the eighth loading stage, the damage indices in elements 4 and 5 becomes 0.41 and 0.55 respectively. Similar discussions apply to the damages in the 16 element model.

Comparison of the identified results from the assessment loads of 10, 17, 25, 35, 45, 50 and 55 kN with those from the assessment load 60 kN shows a difference of 101.32%, 76.83%, 53.48%, 26.60%, 12.02%, 7.29% and 7.43%, respectively. When the assessment load is not smaller than 35 kN, the identified results are acceptable. Although the load that creates the damage is not known in real case, acceptable results can be obtained from any assessment load that falls in the range of the flattened part of the curve.

3.2 Damage identification – simulating practical assessment

The crack damage in the beam after the eighth loading stage was again assessed with loads at different load levels. The beam was unloaded and then loaded again with the assessment loads of 10, 15, 20, 25, 30, 35, 40, 45, 50, 55 and 60 kN in turn. This is equivalent to the common practice of assessing a structure which has been badly damaged under extreme loading with a smaller loading in the assessment. Existing dynamic approaches of assessment are conducted with the structure unloaded. Results from such assessment procedure at different load level smaller than that creates the damage are shown in Figs. 6(c) and 6(d). The damage index for element 4 associated with the damage created at 67 kN is 0.41 and that for element 5 is 0.55.

When the assessment load is smaller than 25 kN, concrete at different cross-sections crack with the embedded reinforcement exposed. Many cracks open up leading to variations in the second moment of inertia of the beam with applied load within this loading range. When the assessment load is larger than 25 kN, most of the tensile strains are taken up at some of the existing cracks for their development into major cracks while new crack occurrence is scarce. The stiffness of the beam is affected mainly by the existing cracks and is thus relatively stable. It was also observed in the experiment that only some of the flexural cracks in the beam are closed after the beam was unloaded. The identified damage indices are therefore smaller at a low loading level when the crack damage was not fully mobilized at this small load level. The identified damage value becomes relatively stable when a load above and close to 25 kN is reached. This illustrates a basic problem encountered with damage detection of reinforced concrete structure with a low load level where the flexural crack and crack damage in the steel-concrete interface will not show up under small load, and they will be fully mobilized only under the load that creates them. Therefore the inclusion of an appropriate proportion of the operation load in the condition assessment would be essential.

4. Discussions

Taking the application of the proposed method to a bridge structure, there are always some design load cases for a bridge deck that would be representive of the operational load of the structure. Also for most of the major bridge structures, there is a static load test before the hand-over of the structure from the contractor to the client. These two types of loading are considered sufficient to cause significant crack damage in the bridge deck with the damage stage falls in the plateau region of Figs. 6(c) and 6(d). These loadings could be considered as responsible for the crack damages in the structure.

For the beam studied, assessment with approximately one-third of the load that create the crack damage, i.e., 25 kN out of 67 kN, gives approximately the same damage index as when using the full load of 60 kN as denoted by the flatten region in Figs. 6(c) and 6(d). This is considered valid only for beams that have sustained some permanent deformation (Law *et al.* 1995). Further studies are required for beams with crack damage created at different load levels.

A dynamics approach of assessment which is very popular nowadays can be performed with the structure virtually unloaded, but large underestimation of the damage extent will incur due to reasons discussed as above, and it should be used with utmost care for the assessment of reinforced concrete structures.

It should be mentioned that all the available static measured information are used in the above studies does not mean an application of a sophisticated method to solve a simply supported beam problem. Every effort is made to ensure the identified results can be shown to be dependent on the load environment of the beam instead of other influencing factors. Beam of other configurations including continuous beams can be similarly treated for the effect of the load the beam carries on their condition assessment.

5. Conclusions

This paper studies the effect of the load carried by a reinforced concrete beam on the final assessment result of the crack damage. The assessment is performed with a static approach. The crack damage is modelled as a crack zone. The identified damage magnitudes from a selected high load level and a low load level are compared. Unlike results obtained for structures of isotropic homogeneous material, the identified damage level of the reinforced concrete beam studied is found dependent on the static load it carries. It may be concluded that accurate assessment of the crack damage in a reinforced concrete beam is only possible when a load similar to the one that creates the damage is used in the identification.

Acknowledgements

The work described in this paper was supported by a University Postdoctoral Research Fellowship

Scheme from the University of Western Australia and a grant from the Hong Kong Polytechnic University Research Funding Project No.G-YW98.

References

Banan, M.R. and Hjelmstad, K.D. (1994), "Parameter estimation of structures from static response. I. Computational aspects", *J. Struct. Eng.*, ASCE, **120**(11), 3243-3258.

Cerri, M.N. and Vestroni, F. (2000) "Detection of damage in beams subjected to diffused cracking", *J. Sound Vib.*, **234**(2), 259-276.

Goldfarb, D. and Idnani, A. (1983), "A numerically stable dual method for solving strictly convex quadratic problems", *Math. Program.*, **27**, 1-33.

Law, S.S., Ward, H.S., Shi, G.B., Chen, R.Z., Waldron, P. and Taylor, C. (1995), "Dynamic assessment of bridge load carrying capacities – II", *J. Struct. Eng.,* ASCE, **121**(3), 488-495.

Maeck, J., Abdel Wahab, M., Peeters, B., De Roeck, G., De Visscher, J., De Wilde, W.P., Ndambi, J.-M. and Vantomme, J. (2000) "Damage identification in reinforced concrete structures by dynamic stiffness determination", *Eng. Struct.*, **22**(10), 1339-1349.

Wahab, M.M., De Roeck, G. and Peeters, B. (1999), "Parameterization of damage in reinforced concrete structures using model updating", *J. Sound Vib.*, **228**(4), 717-730.

Wang, X., Hu, N., Fukunaga, H. and Yao, Z.H. (2001), "Structural damage identification using static test data and changes in frequencies", *Eng. Struct.,* **23**, 610-621.